

Coherent Oscillations in an Exciton-Polariton Josephson Junction

K. G. Lagoudakis,¹ B. Pietka,¹ M. Wouters,² R. André,³ and B. Deveaud-Plédran¹

¹*ICMP, Ecole Polytechnique Fédérale de Lausanne (EPFL), 1015 Lausanne, Switzerland*

²*ITP, Ecole Polytechnique Fédérale de Lausanne (EPFL), 1015 Lausanne, Switzerland*

³*Institut Néel, CNRS, Grenoble, France*

(Received 13 April 2010; published 15 September 2010)

We report on the observation of spontaneous coherent oscillations in a microcavity polariton bosonic Josephson junction. Condensation of exciton polaritons here takes place under incoherent excitation in a double potential well naturally formed in the disorder. Coherent oscillations set on at an excitation power well above the condensation threshold. The time resolved population and phase dynamics reveal the analogy with the ac Josephson effect. A theoretical two-mode model describes the observed effects, explaining how the different realizations of the pulsed experiment can be in phase.

DOI: [10.1103/PhysRevLett.105.120403](https://doi.org/10.1103/PhysRevLett.105.120403)

PACS numbers: 03.75.Lm, 67.85.De, 71.36.+c, 74.50.+r

One of the most striking manifestations of the quantum collective behavior of matter is the Josephson effect: it allows for a classically forbidden current to flow without dissipation [1]. Traditional Josephson junctions are built by means of superconductors separated by thin nonconducting oxide barriers, and they have drawn intense interest for their striking phenomenology. A bosonic analog is the so-called bosonic Josephson junction (BJJ) where two macroscopic populations of bosons are trapped in a double well geometry. Bose Einstein condensation of dilute atomic gases has allowed for the realization of BJJs by trapping two condensates in double wells [2,3]. The Josephson effect results in a flow through classically forbidden barriers and produces an alternating current from a constant potential difference.

The possibility to engineer and dynamically tune atomic condensates has allowed for all the possible regimes and their respective phenomenology to be observed. More specifically in the Josephson regime, the most remarkable phenomena are the ac and dc Josephson effects [4], the macroscopic quantum self-trapping, and the Josephson plasma oscillations [5].

The more recent achievement of condensation of exciton polaritons in semiconductor microcavities [6] has provided a new field of study of quantum phenomena related to the macroscopic phase coherence. Polaritons are bosonic quasiparticles that occur in semiconductor microcavities as a result of the strong coupling between light (cavity photons) and matter excitations (quantum well excitons). Owing to their half-light nature, polaritons have an exceptionally low mass of the order of 10^{-5} the mass of free electrons, which allows for condensation at temperatures easily achievable by cryogenic means. Having a limited lifetime of about 3 psec, they leak out of the microcavity and thus have to be continuously replenished, a process that renders polariton condensates out of equilibrium. It is because of this aspect that polariton condensates provide a very rich phenomenology [7]. Another advantage of this system is that all the polariton properties are imprinted to the emitted lumines-

cence so that one has access to both population and phase by optical imaging and interferometric methods.

Here we have set out to investigate Josephson effects in a BJJ formed by two spatially separated condensates of exciton polaritons in a CdTe microcavity.

The condensate pair is trapped in a naturally occurring disorder double potential well which is formed during the sample growth. These structures tend to appear more frequently in linear disorder valleys; see Fig. 1(a). The sample employed here is the one previously used in our studies [8]. We used pulsed nonresonant excitation at 695 nm with pulse duration ~ 250 fsec, which gives a spectral FWHM of less than 3 nm. The condensate emission at about 740 nm is detected with a streak camera with temporal resolution ~ 3 psec. The Gaussian excitation spot (waist $\sim 15 \mu\text{m}$) was displaced with respect to the center of the BJJ giving imbalanced excitation intensities on the two wells. The population oscillations were revealed by forming the real space image [Fig. 1(a)] on the entrance slits of the streak camera. The BJJ that we studied here, consisted of two wells of about $2 \mu\text{m}$ size each, separated by a barrier of $\sim 0.5 \mu\text{m}$. From the spectroscopic data we estimated the depth of the confining potential to be approximately 3.5 meV below the average polariton energy [9]. Remarkably, the Josephson oscillations only show up above a threshold excitation power $P_{\text{OT}} = 380 \mu\text{W}$ that is higher than the power required for condensation $P_{\text{CT}} = 200 \mu\text{W}$. At powers $P_{\text{CT}} < P < P_{\text{OT}}$, coherence between the two wells is observed, but no population exchange is seen between the two trapped condensates as is evident in Fig. 1(b).

For $P > P_{\text{OT}}$, the behavior changes dramatically and one clearly sees an exchange of particles between the two wells Fig. 1(c). To assess that the polariton currents are driven by the phase difference between the two wells, one needs the relative phase difference $\Delta\theta(t) = \theta_L(t) - \theta_R(t)$ with $\theta_{L,R}$ the absolute condensate phase in the respective wells. To this purpose we used the modified Michelson interferometer in a mirror-retroreflector configuration [6] to interfere

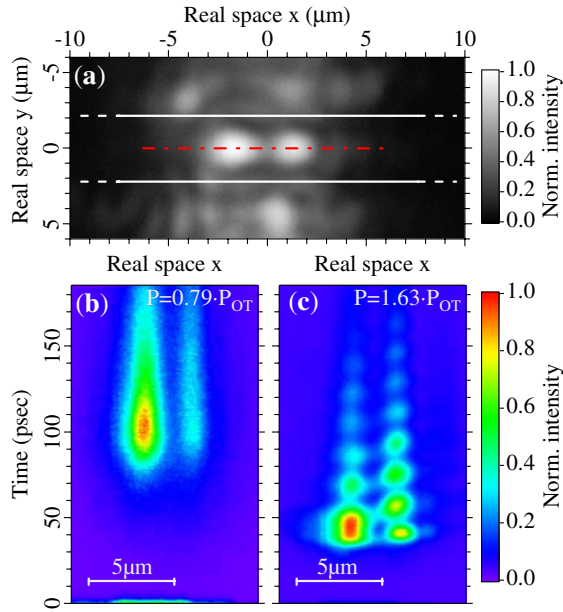


FIG. 1 (color online). (a) Time integrated real space image of the luminescence. The dash-dotted line is the line selected by the streak camera, and the solid lines with dashed edges enclose the linear disorder valley in which the double well potentials are frequent. (b) Time resolved photoluminescence along the dash-dotted line in (a) for $P < P_{OT}$. (c) Same as in (b) but for $P > P_{OT}$. The incident pulse defines the zero time.

the luminescence of the left well with that of the right. The density of fringes in the interferograms is set by the displacement of the retroreflector which adds an angle to the reflected beam after passing through the imaging lens. The resulting interference term is of the form $\cos[k_L x + \Delta\theta(t)]$ with $\Delta\theta(t)$ the relative phase. One directly sees that if the two condensates have a constant phase difference, the fringes are parallel with the time axis [Fig. 2(a)], whereas if their phase increases linearly in time, the fringes appear tilted [Fig. 2(b)]. By scanning the relative phase of the two interferometer arms over 3π we were able to fit the function $A(x, t) \cos[\phi + \Delta\theta(x, t)]$ at each pixel (x, t) and thus retrieve the relative phase $\Delta\theta(x, t)$ up to the unknown constant ϕ induced by the initial position of the interferometer.

The extracted relative phase $\Delta\theta$ and normalized population difference $\Delta N = (N_L - N_R)/(N_L + N_R)$ are shown in Fig. 3. Density and phase oscillations show the expected relation: the measurements are consistent with a Josephson current that flows from the well with the lower phase to the one with higher phase and vanishes when the phase difference is zero. We thus observe density oscillations between two macroscopically occupied polariton states driven by their phase difference, i.e., the bosonic Josephson effect [10]. A closer look at the population dynamics reveals that there is a strong imbalance of the population in the first moments of the oscillations (between 35 and 65 psec) which is due to a higher energy level that does not contribute to the beatings and dies out quickly within the same

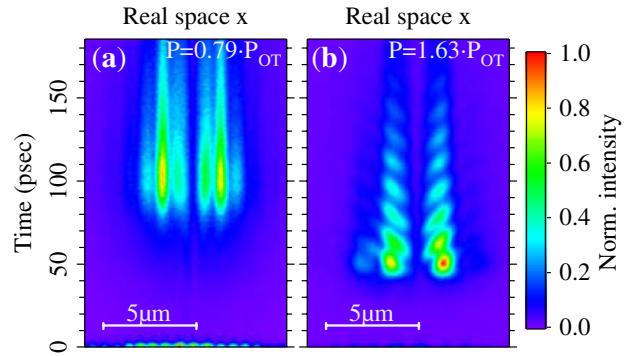


FIG. 2 (color online). Time resolved interferograms along the dash-dotted line of Fig. 1(a) formed by the superposition of the luminescence of the right and left wells. (a) $P < P_{OT}$. The lack of currents is clearly seen with the constant phase relation between the two wells (straight fringes in time). (b) Same as in (a) but for $P > P_{OT}$. The oscillatory current of particles is due to the linearly increasing relative phase in time which provokes the tilting of the fringes.

temporal window. Time integrated spectrally resolved studies revealed the emission lines of the two beating states, their energy difference corresponding to the beating frequency, and the slightly higher energy state that has no oscillatory signature in the temporal response. The frequency of the oscillations is 75.6 GHz, which corresponds to an energy difference of $312 \mu\text{eV}$, a value confirmed by the spectroscopic studies [9].

The relative phase between the two wells is expected to increase linearly in time. Modulo 2π , this should in turn give a perfect sawtooth form of the relative phase evolution from $-\pi$ to π . Contrary to this we observe a smoothed sawtooth phase evolution with much smaller amplitude (-0.3π to 0.3π).

It is actually not trivial that Josephson oscillations can be observed under the present conditions. The pulsed experiment is repeated $>10^6$ of times and starts every time with

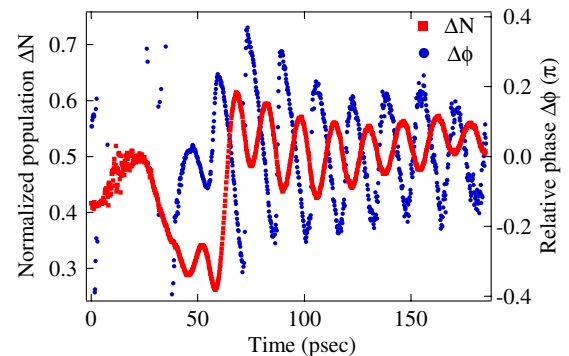


FIG. 3 (color online). Temporal evolution of relative well population and relative well phase. The relative population (squares) oscillates symmetrically around zero, and the phase (circles) is following the population oscillations. A striking feature is that the phase shows small amplitude sawtoothlike oscillations. The region between 5 and 35 psec had a very low overall intensity and thus the relative phase could not be calculated.

an arbitrary relative phase between the condensates in the two disorder minima. One would therefore rather expect to see oscillations in a single run of the experiment, but not in the realization averaged signal.

In order to gain more insight in the origin and nature of Josephson oscillations that we observe, we compare our observations with the predictions of a two-mode model that takes into account the polariton losses and their replenishment from the exciton reservoir [8,11,12]:

$$i\frac{d}{dt}\psi_{L,R} = \left\{ \varepsilon_{L,R} + g_{L,R}|\psi_{L,R}|^2 + \frac{i}{2}[R(n_{R2;L,R}) - \gamma] \right\} \psi_{L,R} + J\psi_{R,L} + \xi_{L,R}. \quad (1)$$

Here, $\varepsilon_{L,R}$ are the energies of the modes in the absence of the tunneling coupling J and γ is the linewidth in the linear regime. The nonresonant excitation enters the polariton dynamics through the stimulated relaxation rate $R(n_{R2})$. The exciton reservoir density n_{R2} consists of the active excitons that fulfill energy and momentum conservation for scattering into the lower polariton branch. Their density is modeled with the rate equation

$$\frac{dn_{R2;L,R}}{dt} = \gamma_{R12} \left(\frac{n_{R1;L,R}}{r_{12}} - n_{R2;L,R} \right) - \gamma_{R2} n_{R2;L,R} - \alpha R(n_{R2;L,R}) |\psi_{L,R}|^2. \quad (2)$$

Here, r_{12} is the steady state ratio between inactive and active excitons. The active exciton density is normalized to be unity at the condensation threshold and α is the depletion factor of this reservoir due to the scattering into the lower polariton branch. The inactive exciton density n_{R1} dynamics is given by

$$\frac{dn_{R1;L,R}}{dt} = \gamma_{R12} \left(\frac{n_{R1;L,R}}{r_{12}} - n_{R2;L,R} \right) - \gamma_{R1} n_{R1;L,R} + P_{L,R}. \quad (3)$$

The noise term ξ models the spontaneous decay and scattering events, and can be explicitly computed within the truncated Wigner approximation [11]. The most important stochastic element is, however, the initial condition of the polariton field: it starts in a vacuum state with random phase.

Figure 4 shows two simulations of the dynamics under pulsed excitation, both above the threshold for condensation, but only for the higher excitation power (right-hand side panels) the Josephson oscillations survive the realization averaging. Our simulations thus reproduce the experimental observation that the threshold for Josephson oscillations P_{OT} is above the one for condensation P_{CT} . Figures 4(a) and 4(b) show multiple realizations of the density or phase evolution for $P_{CT} < P < P_{OT}$. Individual realizations of the density-phase evolution clearly show oscillations. In the average over many runs of the experiment [Fig. 4(c)] these oscillations have, however, disappeared, because the different realizations are not in phase. Only at higher power [see Figs. 4(d)–4(f)] are the

oscillations in phase with each other and they survive the realization averaging.

Theoretically, the emergence of a deterministic relative phase in the early stage of the dynamics only occurs for asymmetric pumping. The physical reason is the following. The dynamics of the relative phase $\Delta\theta(t) = \theta_L(t) - \theta_R(t)$ is governed by

$$\frac{d\Delta\theta}{dt} = J \left(\sqrt{\frac{N_L}{N_R}} - \sqrt{\frac{N_R}{N_L}} \right) \cos(\Delta\theta) + \varepsilon_R - \varepsilon_L + g_R N_R - g_L N_L, \quad (4)$$

where we have introduced the density and phase of the fields $\psi_j = \sqrt{N_j} e^{i\theta_j}$, $j = L, R$. The emergence of a fixed relative phase shortly after the condensate formation can be more easily understood for $\varepsilon_R = \varepsilon_L$. If one of the two densities is much larger than the other one, Eq. (4) implies that the relative phase will be quickly driven to $\Delta\theta = \pi/2$, the zero of the cosine. This dynamics washes out the initial randomness of the relative phase and leads to a subsequent deterministic evolution with Josephson oscillations that are in phase in each realization. A necessary condition for the pump asymmetry to lead to a large density difference on the two wells is that at early times the tunneling currents that transfer particles between the two wells are negligible with respect to the exponential growth. This is only the case at sufficiently high pump power, when in the initial exponential growth stage $R \gg J$.

A second question we can address with our model is whether our observations are rather related to the Josephson plasma oscillations or the ac Josephson effect. The latter effect is driven by the energy difference between the two potential minima, while the former originates from an initial condition that is different from the steady state. A previous study [13] of plasma oscillations in a nonequilibrium polariton condensate under continuous wave excitation has shown that plasma oscillations feature a damped sinusoidal dynamics, in contrast to the persistent sawtooth-like behavior that is observed in our experiments. The polariton analog of the ac Josephson effect, on the other hand, occurs when the energy difference between the two wells is too big for a synchronized solution to exist [14,15]. The beatings between the two modes are responsible for persistent density oscillations and a sawtooth phase profile, as we observe in our experiments. The oscillations between two wells with different frequency condensates are entirely analogous to the ac Josephson oscillations where the difference in chemical potential is imposed by an external voltage.

An unexpected feature of the sawtooth oscillations in Fig. 3 is that their amplitude is much below the expected 2π . This property of the realization averaged phase can be traced back to the fact that the phase evolution is steeper for large $\Delta\theta$ [see Fig. 4(d)]. As a consequence, large values of $\Delta\theta$ do not contribute much to the average phase difference. The physical reason is that large phase differences go together with a low population in one of the two wells.

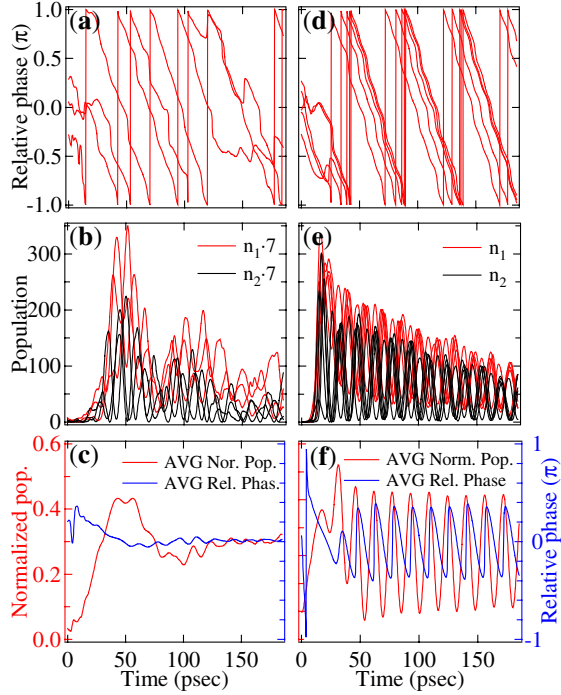


FIG. 4 (color online). Theoretical simulations. (a) Phase evolution for individual realizations for low excitation powers. (b) Populations in left [gray (red) line] and right (black line) well for the three realizations of (a). (c) Averaged relative phase modulo 2π and normalized populations from (a),(b). Panels (d)–(f) are the same as panels (a)–(c), only this time for excitation intensity above the oscillation threshold. Both the phase and the populations have very similar behaviors for different realizations demonstrating the effect of the phase-locking mechanism. The non-negligible fluctuations of the phase are the reason for the smoothed sawtooth phase profile [19].

When one of the populations becomes very small, the Josephson current quickly reverts so to replenish it. A further consequence of the rapid phase variation is that the shot to shot variations are more significant at those times. This results in a reduced coherence, seen both in the experiments and the theoretical simulations (not shown in the figures).

Finally, our two-mode model also allows us to understand the role of the polariton-polariton interactions on the Josephson oscillations. In the absence of interactions, the oscillation frequency is set by the detuning and tunneling coupling. When the blueshift due to polariton-polariton interactions $\mu_j = gN_j$ becomes comparable to the detuning $\Delta\varepsilon$, interactions make the oscillation frequency increase for increasing pump intensity. Contrary to this, in experiments a slight decrease of the frequency is observed. We therefore conclude that polariton-polariton interactions have a negligible effect on the oscillation dynamics and that our polaritonic BJJ is in the so-called Rabi regime [16]. The slight decrease in oscillation frequency can be reproduced in the theory when taking into account the interactions between the polaritons and the exciton reservoir.

In this Letter we have provided experimental evidence of coherent oscillations in a polaritonic Josephson junction. We have shown simultaneous existence of population and phase oscillations. The persistent sawtoothlike phase oscillations are the polariton analog of the ac Josephson effect. Theory shows that the Josephson oscillations survive the realization averaging, with reduced amplitude, despite the random initial phase thanks to a spontaneous synchronization mechanism above a critical pump intensity. The present realization of the Josephson effect relied on the accidental presence of coupled wells in our disordered microcavity. Controlled growth of polariton traps with mesa structures [17] and micropillars [18] will allow for a more systematic analysis of the different regimes of Josephson oscillations, where polariton-polariton interactions can play a more pronounced role.

The authors wish to thank Le Si Dang, V. Savona, Y. Leger, I. Carusotto, D. Sarchi, M. Richard, and A. Baas for stimulating discussions. The work was supported by the Swiss National Research Foundation through NCCR “Quantum Photonics.”

- [1] A. Barone and G. Paterno, *Physics and Applications of the Josephson Effect* (Wiley-Interscience, New York, 1982).
- [2] F. S. Cataliotti *et al.*, *Science* **293**, 843 (2001).
- [3] R. Gati *et al.*, *Appl. Phys. B* **82**, 207 (2006).
- [4] S. Levy *et al.*, *Nature (London)* **449**, 579 (2007).
- [5] M. Albiez *et al.*, *Phys. Rev. Lett.* **95**, 010402 (2005).
- [6] J. Kasprzak *et al.*, *Nature (London)* **443**, 409 (2006).
- [7] I. Carusotto *et al.*, *Phys. Rev. Lett.* **103**, 033601 (2009).
- [8] G. Nardin *et al.*, *Phys. Rev. Lett.* **103**, 256402 (2009).
- [9] See supplementary material at <http://link.aps.org/supplemental/10.1103/PhysRevLett.105.120403> for the time integrated spectroscopic data.
- [10] J. Javanainen, *Phys. Rev. Lett.* **57**, 3164 (1986).
- [11] M. Wouters and V. Savona, *Phys. Rev. B* **79**, 165302 (2009).
- [12] J. Keeling and N. G. Berloff, *Phys. Rev. Lett.* **100**, 250401 (2008).
- [13] M. Wouters and I. Carusotto, *Phys. Rev. Lett.* **99**, 140402 (2007).
- [14] M. Wouters, I. Carusotto, and C. Ciuti, *Phys. Rev. B* **77**, 115340 (2008).
- [15] M. O. Borgh, J. Keeling, and N. G. Berloff, *Phys. Rev. B* **81**, 235302 (2010).
- [16] R. Gati and M. K. Oberthaler, *J. Phys. B* **40**, R61 (2007).
- [17] O. El Daif *et al.*, *Appl. Phys. Lett.* **88**, 061105 (2006).
- [18] J. Bloch *et al.*, *Superlattices Microstruct.* **22**, 371 (1997).
- [19] In the reported simulations, the parameters were taken as $\Delta\varepsilon/\gamma = 2$, $J/\gamma = 0.5$, $\gamma_{R1} = \gamma_{R2} = 0.01\gamma$, $\gamma_{R12} = 0.1\gamma$, $r_{12} = 10$, $\alpha = 0.01$, $g_{R,L} = 0$, and $\hbar\gamma = 0.45$ meV. The pulsed excitation is modeled with an initial density for the first reservoir $n_{R1:L} = 26$, $n_{R1:R} = 19$ for $P < P_{OT}$ and $n_{R1:L} = 105$, $n_{R1:R} = 75$ for $P > P_{OT}$. Numerical results were obtained by Monte Carlo averaging over 1000 realizations over the initial conditions and the noise.